Petersson, A., Kemp, A.I.S., and Whitehouse, M.J., 2019, A Yilgarn seed to the Pilbara Craton (Australia)? Evidence from inherited zircons: Geology, v. 47, https://doi.org/10.1130/G46696.1

SAMPLE LOCATIONS

Sample name	UTM Zone	UTM Easting	UTM Northing
15TKPB17	50K	748275	7646526
18APPB12	50K	747991	7646382
18APPB13	50K	748044	7646393
18APPB16	50K	750833	7646782

ANALYTICAL METHODS

Major And Trace-Element Analyses

Two of the samples (15TKPB17 and 18APPB16) were analysed by Bureau Veritas Minerals Pty Ltd in Perth. The samples were cast using a 66:34 (Lithium Tetraborate 66% / Lithium Metaborate 34%) flux with 4% Lithium nitrate added to form a glass bead. Major elements were determined by X-Ray Fluorescence. Trace elements were determined by Laser Ablation Inductively Coupled Plasma Mass Spectrometry on a fused bead. Loss on Ignition was determined using a robotic TGA system with furnaces set to 110°C and 1000°C (LOI1000). A sub-sample was digested with sulphuric and hydrofluoric acids and FeO determined via titration. Accuracy and precision of the analyses were monitored using geochemical reference rock powders (Kerba Monzogranite and Bunbury Basalt; Morris, 2007), inserted as unknown samples. All major and trace element data, including that obtained from the reference materials, are found in Supplementary table DR2.

Zircon U–Pb SIMS Age Determination

Nordsim

Secondary ion mass spectrometry (SIMS) U–Th–Pb isotopic analyses were performed using a large geometry Cameca IMS1280 mass spectrometer at the Swedish Museum of Natural History. The instrument set up follows that of Whitehouse et al. (1999), Whitehouse and Kamber (2005) and references therein. An O_2^- primary beam with 23 kV incident energy (−13 kV primary, +10 kV secondary) was used for sputtering. For this study, the primary beam was operated in aperture illumination (Köhler) mode yielding a ~15–20 μm spot. Pre-sputtering with a 25 μm raster for 120 s, centring of the secondary ion beam in the 3000 μm field aperture (FA), mass calibration optimisation, and optimisation of the secondary beam energy distribution was performed automatically for each run, FA, and energy adjustment using the $^{90}Zr_2{}^{16}O^+$ species at nominal mass 196. Mass calibration of all peaks in the mono-collection sequence was performed at the start of each session; within run mass calibration optimisation was performed using the $^{90}Zr_2{}^{16}O^+$ peak, applying a shift to all other species. A mass resolution (M/ΔM) of ~5400 was used to ensure adequate separation of Pb isotope peaks from nearby $HfSi^+$ species. Ion signals were detected using the axial ion-counting electron multiplier. All analyses were run in fully automated chain sequences. Data reduction

assumes a power law relationship between Pb^+/U^+ and UO_2^+/U^+ratios with an empirically derived slope in order to calculate actual Pb/U ratios based on those in the 91500 standard. U concentration and Th/U ratio are also referenced to the 91500 standard. Common Pb correction is made if the ^{204}Pb signal statistically exceeds average background and assumes a $^{207}Pb/^{206}Pb$ ratio of 0.83 (equivalent to present day Stacey and Kramers, 1975, model terrestrial Pb). Decay constants follow the recommendations of Jaffey et al., (1971) and compiled by Steiger and Jäger (1977). All age calculations were done in Isoplot 4.15 (Ludwig, 2008) and quoted at 2σ uncertainty level. All internal errors and external uncertainty in the standard analyses are propagated. Systematic uncertainties highlighted by interlaboratory experiments are not propagated. All results are presented in Supplementary table DR1.

Curtin SHRIMP

Zircon ion microprobe dating on the SHRIMP II at Curtin University, Perth, follow the methodology of De Laeter and Kennedy (1998), Kennedy and De Laeter (1998), and Nelson et al. (1997). All zircon U–Pb isotope data is presented in Supplementary table DR1. All $^{207}Pb/^{206}Pb$ zircon ages referred to in this study have been corrected for common Pb, assuming a composition of common Pb following Compston et al. (1984). Reference zircon M257 ($^{206}Pb/^{238}U$ age = 561.3 ± 0.6 Ma; Nasdala et al., 2008) was used as primary standard and OGC zircons ($^{207}Pb/^{206}Pb$ age = 3465.4 ± 0.6 Ma, Stern et al., 2009) were routinely analyzed to monitor analytical precision and accuracy of $^{207}Pb/^{206}Pb$. All SHRIMP U–Pb data were reduced via the software packages Isoplot and Squid (Ludwig, 2008; 2009).

Ion Microprobe Oxygen Isotope Analysis In Zircon

Oxygen isotope ratios ($^{18}O/^{16}O$) in zircon were determined using a Cameca IMS 1280 multi-collector ion microprobe hosted by the Centre for Microscopy, Characterisation and Analysis (CMCA), University of Western Australia (UWA). After U–Pb analyses, Au-coating was removed using a light polishing. The sample mounts were then carefully cleaned with detergent, distilled water and ethanol in an ultrasonic bath and re-coated with gold (30nm in thickness) prior to SIMS O isotope analyses.

The sample surface is sputtered over a 10 x 10 μm area with a 10 kV, Gaussian Cs^+ beam with an intensity of ~3 nA and total impact energy of 20 keV. An electron gun is used to ensure charge compensation during the analyses. Secondary ions were admitted in the double focusing mass spectrometer within a 110 μm entrance slit and focused in the centre of a 4000 μm field aperture (x 100 magnification). They are energy filtered using a 30 eV band pass with a 5 eV gap toward the high-energy side. ^{16}O and ^{18}O are collected simultaneously in Faraday cup detectors fitted with 10^{10} Ω (L'2) and 10^{11} Ω (H1) resistors, respectively, and operating at a mass resolution of ~2430. The magnetic field was regulated using NMR control.

Each analysis includes a pre-sputtering over a 15 x 15 μm area during 30s and the automatic centring of the secondary ions in the field aperture, contrast aperture and entrance slit. Each analysis then consists of 20 four-second cycles, which give an average internal precision of ~0.16‰ (2 SE). The analytical session was monitored in terms of drift using at least two bracketing standards every 5 to 6 sample analyses. Instrumental mass fractionation (IMF) was corrected using Temora 2 (8.2 ‰; Black et al., 2004) following the procedures described in Kita et al. (2009). The spot-to-spot reproducibility was 0.2-0.3‰ (2 SD) on Temora 2 during the analytical session. Two extra zircon references were used for quality control, Penglai (n=26, weighted mean $^{18}O/^{16}O$=0.0020154±0.0000001, reference $^{18}O/^{16}O$=0.0020158±0.0000002 (Li et al., 2010) and OGC/OG1 (n=32, weighted mean

$^{18}O/^{16}O$=0.0020171±0.0000001, reference $^{18}O/^{16}O$=0.0020170±0.0000001 (Petersson et al., 2019). Uncertainty on each $\delta^{18}O$ spot has been calculated by propagating the errors on instrumental mass fractionation determination, which include the standard deviation of the mean oxygen isotope ratio measured on the primary standard during the session, and internal error on each sample data point. Raw $^{18}O/^{16}O$ ratios and corrected $\delta^{18}O$ (quoted with respect to Vienna Standard Mean Ocean Water or VSMOW) are found in Supplementary table DR3 and DR4.

LA-MC-ICP-MS Zircon Lu–Hf Analyses

Lu–Hf analyses were carried out at the School of Earth Sciences at The University of Western Australia using a 193 nm Cetac Analyte G2 excimer laser installed with a two-volume HelEx2 sample cell, and a Thermo-Scientific Neptune Plus High-Resolution Multicollector ICP-MS.

Lu–Hf spot overlapped pits from both the U–Pb and O isotope analysis wherever possible. Circular spots with a diameter of 40–50 μm were used. Each analysis was initiated by a 30 s electronic baseline followed by an ablation sequence of 60 s comprising 60 integration cycles of one second each. A laser pulse repetition rate of 4 Hz was used and the laser energy was held at ~5 J/cm^2, which equals an ablation rate of ~0.05 μm per pulse for zircon. Helium carrier gas (1.0 l/min) was used to transport the ablated particles from the sample chamber. This was combined with argon gas (flow rate c. 0.6 l/min) and nitrogen (~0.012 l/min) further downstream before entering the argon plasma. Masses ^{171}Yb, ^{173}Yb, ^{175}Lu, ^{176}(Hf+Lu+Yb), ^{177}Hf, ^{178}Hf, ^{179}Hf and ^{180}(Hf+W+Ta) were measured simultaneously by Faraday detectors. Isobaric interference of ^{176}Yb and ^{176}Lu on ^{176}Hf was calculated using the measured intensities of ^{171}Yb and ^{175}Lu along with known isotopic ratios of $^{176}Yb/^{171}Yb$=0.897145 (Segal et al., 2003) and $^{176}Lu/^{175}Lu$=0.02655 (Vervoort et al., 2004). Mass bias corrections were calculated using the exponential law. For calculations of βHf, measured intensities of ^{179}Hf and ^{177}Hf and a $^{179}Hf/^{177}Hf$ ratio of 0.7325 was used. βYb was calculated using measured intensities of ^{173}Yb and ^{171}Yb and a $^{176}Yb/^{171}Yb$ ratio of 1.130172 (Segal et al., 2003). Mass bias behaviour of Lu was assumed to be identical to Yb. Four zircon references were used for quality control, FC-1 ($^{176}Hf/^{177}Hf$=0.282179±0.000019 at 2 SD, n=16, weighted average $^{176}Hf/^{177}Hf$=0.282179±0.000005 at 95% conf. MSWD=0.9; solution value 0.282184±0.000016), Mud Tank zircon ($^{176}Hf/^{177}Hf$=0.282491±0.000011, n=26, weighted average $^{176}Hf/^{177}Hf$=0.282490±0.000003 at 95% conf. MSWD=1.8; solution value 0.282507±0.000006, Temora 2 ($^{176}Hf/^{177}Hf$=0.282683±0.000020, n=3; weighted average $^{176}Hf/^{177}Hf$=0.282683±0.000011 at 95% conf. MSWD=0.3; solution value 0.282686±0.000008), 91500 ($^{176}Hf/^{177}Hf$=0.282305±0.000023, n=8; weighted average $^{176}Hf/^{177}Hf$=0.282306±0.000008 at 95% conf. MSWD=0.6; solution value 0.282306±0.000008, Woodhead and Hergt, 2005) and OGC ($^{176}Hf/^{177}Hf$=0.280635±0.000020, n=15; weighted average $^{176}Hf/^{177}Hf$=0.280633±0.000014 at 95% conf. MSWD=6.2; solution value 0.280633±0.000034, Kemp et al., 2017). Age-corrected $^{176}Hf/^{177}Hf_{(3.467\ Ga)}$ for the high $^{176}Lu/^{177}Hf$ zircon yields a weighted mean of $^{176}Hf/^{177}Hf$ =0.280557±0.000005, at 95% conf., MSWD=0.6, within errors identical to the solution value $^{176}Hf/^{177}Hf$ =0.280554±0.000007 of Kemp et al., (2017). Analysed $^{176}Hf/^{177}Hf$ ratios of the sample zircon were normalised based on a comparison between the mean of analysed $^{176}Hf/^{177}Hf$ ratios of Mud Tank zircon measured in a given session and its reported $^{176}Hf/^{177}Hf$ ratio of 0.282507 determined by solution analysis (Woodhead and Hergt, 2005) and itself reported relative to JMC475 $^{176}Hf/^{177}Hf$ = 0.282160). Calculations of εHf were done using $\lambda^{176}Lu=1.867\times10^{-11}$ yr^{-1} (Scherer et al., 2001; Söderlund et al., 2004), ($^{176}Lu/^{177}Hf$)CHUR=0.0336 and ($^{176}Hf/^{177}Hf$)CHUR=0.282785±11 (Bouvier et al., 2008). All zircon Lu–Hf data is found in Supplementary table DR5 and DR6.

References

Black, L.P., Kamo, S.L., Allen, C.M., Davis, D.W., Aleinikoff, J.N., Valley, J.W., Mundil, R., Campbell, I.H., Korsch, R.J.,Williams, I.S., and Foudoulis, C., 2004, Improved $^{206}Pb/^{238}U$ microprobe geochronology by the monitoring of a trace-element-related matrix effect; SHRIMP, ID–TIMS, ELA–ICP–MS and oxygen isotope documentation for a series of zircon standards: Chemical Geology, v. 205, p. 115–140. https://doi.org/10.1016/j.chemgeo.2004.01.003

Bouvier, A., Vervoort, J.D., and Patchett, P.J., 2008, The Lu-Hf and Sm-Nd isotopic composition of CHUR: constraints from unequilibrated chondrites and implication for the bulk composition of terrestrial planets: Earth and Planetary Science Letters, v. 273, p. 48–57. https://doi.org/10.1016/j.epsl.2008.06.010

Compston, W., Williams, I.S., and Meyer, C., 1984, U-Pb geochronology of zircons from lunar breccia 73217 using a sensitive high mass-resolution ion microprobe: Journal of Geophysical Research: Solid Earth, v. 89, p. B525–B534. https://doi.org/10.1029/JB089iS02p0B525

De Laeter, J.R., and Kennedy A.K., 1998, A double focusing mass spectrometer for geochronology: International Journal of Mass Spectrometry, v. 78, p. 43–50. https://doi.org/10.1016/S1387-3806(98)14092-7

Jaffey, A.H., Flynn, K.F., Glendenin, L.E., Bentley, W.T., and Essling, A.M., 1971, Precision measurement of half-lives and specific activities of U 235 and U 238: Physical Review C, 4(5), p.1889. https://doi.org/10.1103/PhysRevC.4.1889

Kemp, A.I., Vervoort, J.D., Bjorkman, K.E., and Iaccheri, L.M., 2017, Hafnium Isotope Characteristics of Palaeoarchaean Zircon OG1/OGC from the Owens Gully Diorite, Pilbara Craton, Western Australia: Geostandards and Geoanalytical Research, v. 41, 659–673. https://doi.org/10.1111/ggr.12182

Kennedy, A.K., and de Laeter, J.R., 1994, The performance characteristics of the WA SHRIMP II ion microprobe. In: Eight International Conference on Geochronology, Cosmochronology and Isotope Geology. Berkley, USA. Abstracts Vol., U.S. Geological Survey Circular, v. 1107, p. 166.

Kita, N.T., Ushikubo, T., Fu, B., and Valley, J.W., 2009, High precision SIMS oxygen isotope analysis and the effect of sample topography: Chemical Geology, v. 264, p. 43–57. https://doi.org/10.1016/j.chemgeo.2009.02.012

Li, X.H., Long, W.G., Li, Q.L., Liu, Y., Zheng, Y.F., Yang, Y.H., Chamberlain, K.R., Wan, D.F., Guo, C.H., Wang, X.C., and Tao, H., 2010, Penglai zircon megacrysts: a potential new working reference material for microbeam determination of Hf–O isotopes and U–Pb age: Geostandards and Geoanalytical Research, v. 34(2), p.117–134. https://doi.org/10.1111/j.1751-908X.2010.00036.x

Ludwig, K.R., 2008, Isoplot 3.70. A Geochronological Toolkit for Microsoft Excel: Berkeley Geochronology Center Special Publications, pp. 4.

Ludwig, K.R., 2009, SQUID II., a user's manual, Berkeley Geochronology Center: Special Publication 2, 2455 Ridge Road, Berkeley, CA 94709, USA 22.

Morris, PA, 2007, Composition of the Bunbury basalt (BB1) and Kerba Monzogranite (KG1) geochemical reference materials, and assessing the contamination effects of mill heads: Geological Survey of Western Australia, Record 2007/14, 22p.

Nasdala, L., Hofmeister, W., Norberg, N., Martinson, J.M., Corfu, F., Dörr, W., Kamo, S.L., Kennedy, A.K., Kronz, A., Reiners, P.W., Frei, D., Kosler, J., Wan, Y., Götze, J., Häger, T., Kröner, A., and Valley, J.W., 2008, Zircon M257 - a Homogeneous Natural Reference Material for the Ion Microprobe U-Pb Analysis of Zircon: Geostandards and Geoanalytical Research, v. 32, p. 247–265. https://doi.org/10.1111/j.1751-908X.2008.00914.x

Nelson, D.R., 1997, Compilation of SHRIMP U-Pb zircon geochronology data, 1996. Geological Survey of Western Australia Record No. 1997/2.

Petersson, A., Kemp, A.I., Hickman, A.H., Whitehouse, M.J., Martin, L., and Gray, C.M., 2019, A new 3.59 Ga magmatic suite and a chondritic source to the east Pilbara Craton: Chemical Geology, v. 511, p. 51–70. https://doi.org/10.1016/j.chemgeo.2019.01.021

Scherer, E., Münker, C., and Mezger, K., 2001, Calibration of the lutetium-hafnium clock: Science, v. 293, p. 683–687. http://doi.org/10.1126/science.1061372

Segal, I., Halicz, L., and Platzner, I.T., 2003, Accurate isotope ratio measurements of ytterbium by multiple collector inductively coupled plasma mass spectrometry applying erbium and hafnium in an improved double external normalization procedure: Journal of Analytical Atomic Spectrometry, v. 18, p. 1217–1223. https://doi.org/10.1039/B307016F

Stacey, J.S., and Kramers, J.D., 1975, Approximation of terrestrial lead isotope evolution by a 2-stage model: Earth and Planetary Science Letters, v, 26, p. 207–221. https://doi.org/10.1016/0012-821X(75)90088-6

Steiger, R.H., and Jäger, E., 1977, Subcommission on geochronology: convention of the use of decay constants in geo- and cosmochronology: Earth and Planetary Science Letters, v. 36, p. 359–362. https://doi.org/10.1016/0012-821X(77)90060-7

Stern, R.A., Bodorkos, S., Kamo, S.L., Hickman, A.H., and Corfu, F., 2009, Measurement of SIMS Instrumental Mass Fractionation of Pb Isotopes During Zircon Dating: Geostandards and Geoanalytical Research, v. 33, p. 145–168, http://doi.org/10.1111/j.1751-908X.2009.00023.x.

Söderlund, U., Patchett, P.J., Vervoort, J.D., and Isachsen, C.E., 2004, The 176Lu decay constant determined by Lu-Hf and U–Pb isotope systematics of Precambrian mafic instrusions: Earth and Planetary Science Letters, v. 219, p. 311–324. https://doi.org/10.1016/S0012-821X(04)00012-3

Vervoort, J.D., Patchett, P.J., Söderlund, U., and Baker, M., 2004, Isotopic composition of Yb and the determination of Lu concentrations and Lu/Hf ratios by isotope dilution using MC-ICPMS. Geochemistry, Geophysics, Geosystems, v. 5(11). https://doi.org/10.1029/2004GC000721

Whitehouse, M.J., Kamber, B.S., and Moorbath, S., 1999, Age significance of U–Th–Pb zircon data from early Archean rocks of west Greenland – a reassessment based on combined ion microprobe and imaging studies: Chemical Geology, v. 160, p. 210–224. https://doi.org/10.1016/S0009-2541(99)00066-2

Whitehouse, M.J., and Kamber, B.S., 2005, Assigning dates to thin gneissic veins in high-grade metamorphic terranes: a cautionary tale from Akilia, Southwest Greenland: Journal of Petrology, v. 46, p. 291–318. https://doi.org/10.1093/petrology/egh075

Woodhead, J.D., and Hergt, J.M., 2005, A preliminary appraisal of seven natural zircon reference materials for in situ Hf isotope determination: Geostandards and Geoanalytical Research, v. 29, p. 183–195. https://doi.org/10.1111/j.1751-908X.2005.tb00891.x

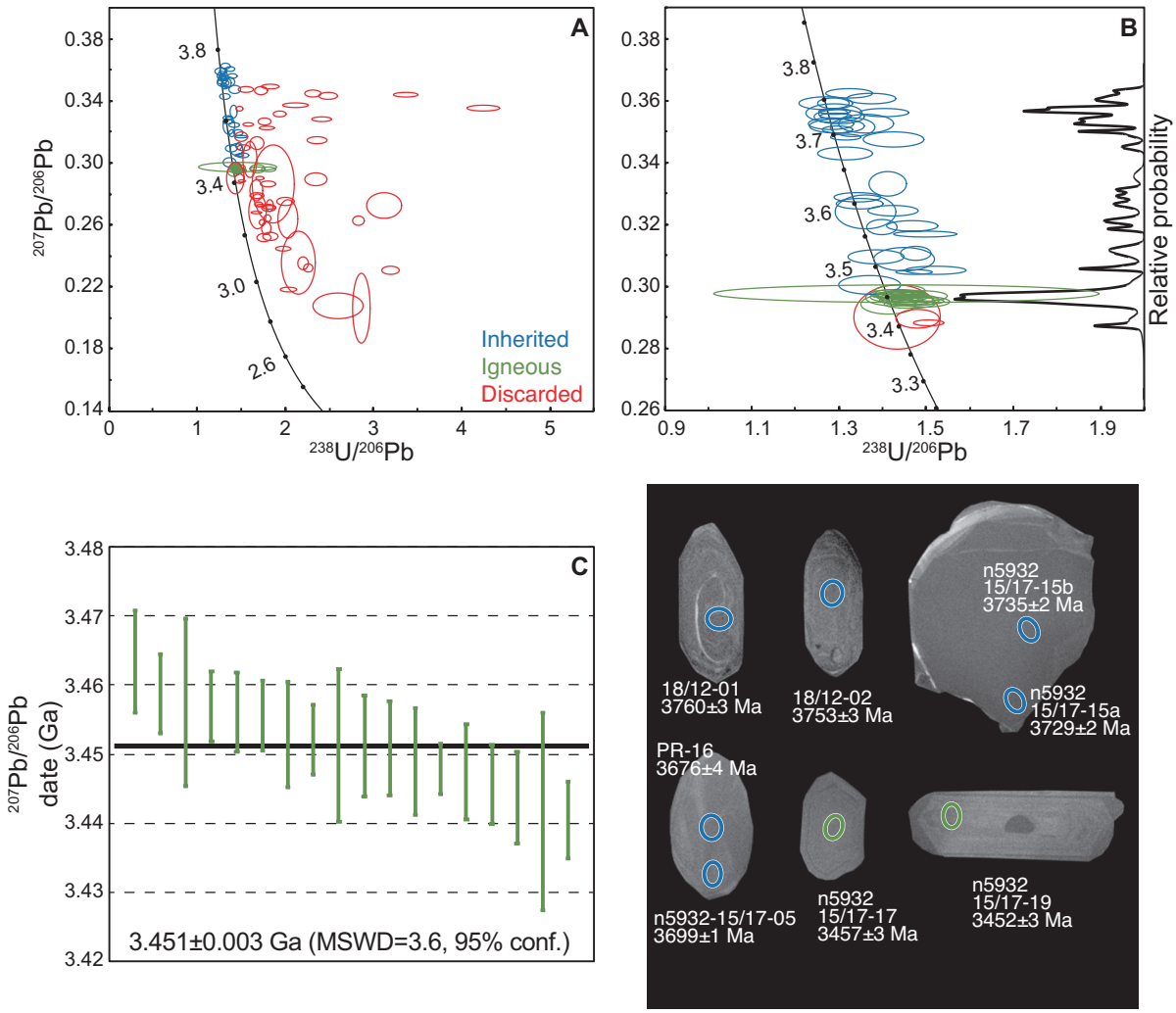

Fig. DR1 A: Tera-Wasserburg diagrams showing SIMS (Secondary-Ion-Mass-Spectrometry) zircon spot data for all zircon U–Pb analyses. B: Ellipses denote all <10% discordant zircon U–Pb analyses. C: $^{207}Pb/^{206}Pb$ weighted mean of igneous grains. Lower right panel: Cathodoluminescence (CL) images of representative zircon grains. Ellipses indicate SIMS spot locations for U–Pb. Blue denote inherited, green denote igneous and red denote discarded analysis.

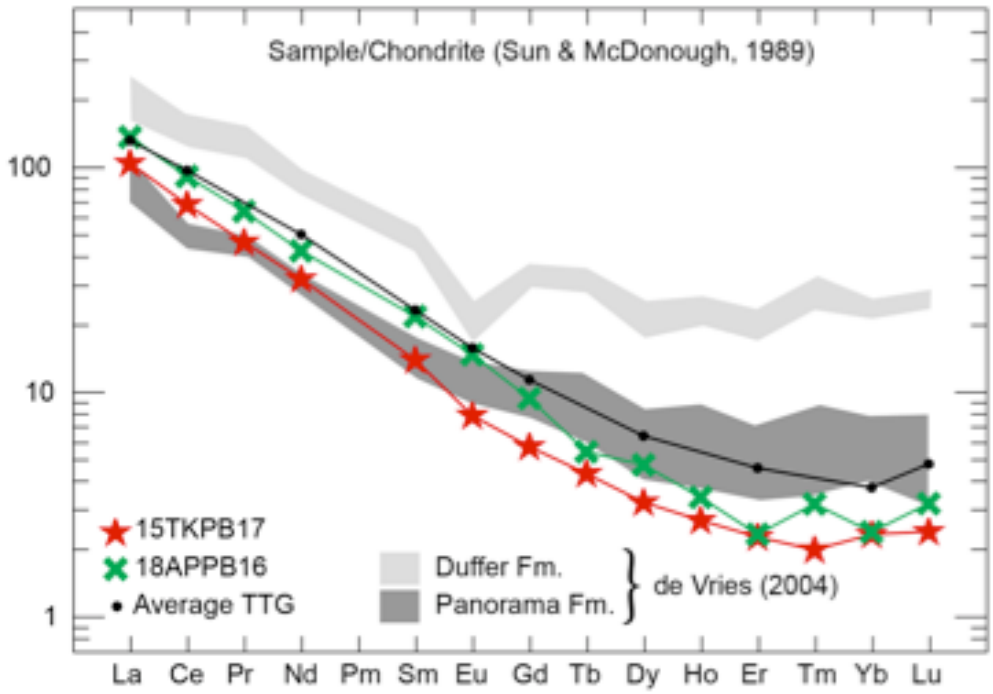

Fig. DR2 The majority of Panorama Ridge is actually mapped as Duffer Formation on the latest map published by the Geological survey of Western Australia (Hickman, 2012). There seem to be a statistically reliable difference in age between the two units where the Duffer Formation is dated to 3.474–3.463 Ga (McNaughton et al. 1993; Nelson 2001) and the ca. 3.458–3.428 Ga (Thorpe et al. 1992; Nelson 1998) age of the Panorama Formation, here constrained to 3.451 ±3 Ma. Hickman
(1983) argued that, similarly to pre- and post-tectonic granitic rocks, the Duffer and Whyman Formations differ in that the Duffer formation is dacitic while the Whyman formation is rhyolitic. Similarly, De Vries (2004) pointed out a few key differences in REE patterns between the Duffer and Panorama formations, where the Duffer dacites have Eu-anomalies and virtually flat HREE (Gd–Lu), while the Panorama Formation rhyodacites have lower REE abundances and lack an Eu-anomaly. The REE signature of the samples in this study confirm a Panorama Formation affiliation (DR2). Further, the new and improved age presented here reinforces a Panorama formation association to the sampled unit.

De Vries, S.T., 2004. Early Archaean sedimentary basins: depositional environment and hydrothermal systems (Doctoral dissertation, University Utrecht). http://dspace.library.uu.nl/handle/1874/1155

Hickman, A.H., 1983. Geology of the Pilbara Block and its environs. West. Aust. Geol. Surv. Bull. 127, 268p.

McNaughton, N.J., Compston, W. and Barley, M.E., 1993. Constraints on the age of the Warrawoona Group, eastern Pilbara block, Western Australia. Precambrian Research, 60(1-4), pp.69-98. https://doi.org/10.1016/0301-9268(93)90045-4

Nelson, D.R., 2001, Compilation of geochronology data, 2000: Geological Survey of Western Australia Record 2001/2, 205 p.

Nelson, D.R., 1998, Compilation of SHRIMP U-Pb zircon geochronology data, 1997: Geological Survey of Western Australia Record 1998/2, 242 p.

Thorpe, R.I., Hickman, A.H., Davis, D.W., Mortensen, J.K. and Trendall, A.F., 1992. U–Pb zircon geochronology of Archaean felsic units in the Marble Bar region, Pilbara Craton, Western Australia. Precambrian Research, 56(3-4), pp.169-189. https://doi.org/10.1016/0301-9268(92)90100-3

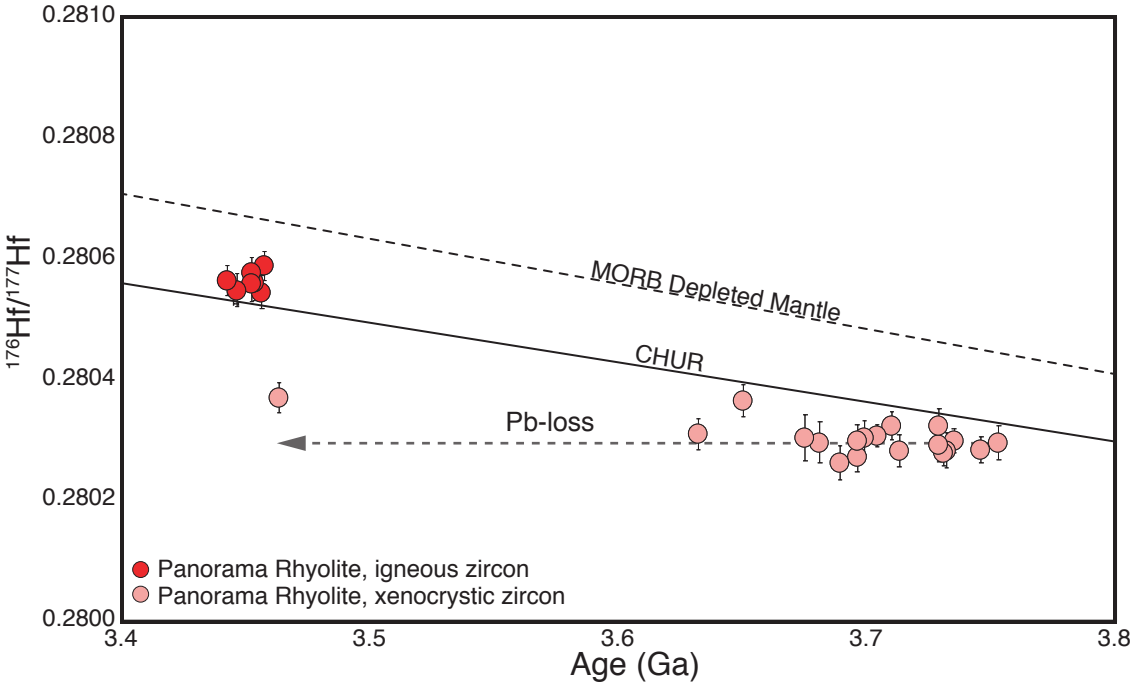
0.2810
0.2808
0.2806
0.2804
0.2802
0.2800
176Hf/177Hf
MORB Depleted Mantle
CHUR
Pb-loss
Panorama Rhyolite, igneous zircon
Panorama Rhyolite, xenocrystic zircon
3.4
3.5
3.6
3.7
3.8
Age (Ga)

Fig. DR3

Table A1. Zircon U–Pb isotopes

Sample ID / Spot #	Sample name	Session	U	Th	Th/U	f_{206} [†]	$^{206}Pb/^{238}U$	±s	$^{207}Pb/^{206}Pb$	±s	Disc. [§]	$^{207}Pb/^{206}Pb$	±s
			(ppm)	(ppm)	(calc.)	(%)		(%)	(corrected)	(%)	(%)	(Ma)	
PR-01	15TKPB17	SHRIMP #1	300	133	0.44	0.07	0.596	±1.93	0.31286	±0.53	18.5	3535	±8
PR-02	15TKPB17	SHRIMP #1	520	82	0.16	0.07	0.666	±1.90	0.31707	±0.40	9.5	3556	±6
PR-03	15TKPB17	SHRIMP #1	143	69	0.48	0.03	0.687	±12.41	0.29754	±0.39	3.2	3457	±6
PR-04b	15TKPB17	SHRIMP #1	120	82	0.68	0.21	0.730	±2.12	0.30055	±0.42	-2.1	3473	±7
PR-05	15TKPB17	SHRIMP #1	266	95	0.36		0.787	±1.96	0.35900	±0.24	0.0	3746	±4
PR-06	15TKPB17	SHRIMP #1	386	84	0.22	0.07	0.734	±1.91	0.35251	±0.33	6.0	3718	±5
PR-07	15TKPB17	SHRIMP #1	1064	595	0.56	0.28	0.505	±1.85	0.24485	±0.26	20.0	3152	±4
PR-08	15TKPB17	SHRIMP #1	627	396	0.63	0.12	0.553	±1.87	0.27107	±0.31	17.7	3312	±5
PR-09	15TKPB17	SHRIMP #1	1333	437	0.33	0.11	0.490	±1.85	0.21824	±0.24	16.2	2968	±4
PR-10	15TKPB17	SHRIMP #1	212	86	0.41	0.11	0.701	±1.99	0.34743	±0.28	9.5	3696	±4
PR-11	15TKPB17	SHRIMP #1	102	44	0.43	0.23	0.426	±2.16	0.28940	±0.58	39.1	3414	±9
PR-12	15TKPB17	SHRIMP #1	438	177	0.40	0.04	0.657	±1.90	0.30966	±0.22	9.6	3519	±3
PR-13	15TKPB17	SHRIMP #1	436	110	0.25	0.10	0.555	±1.95	0.28649	±0.27	20.2	3399	±4
PR-14	15TKPB17	SHRIMP #1	748	366	0.49	0.08	0.598	±1.87	0.28234	±0.98	13.2	3376	±15
PR-15	15TKPB17	SHRIMP #1	269	66	0.24	0.10	0.625	±1.95	0.30199	±1.56	12.8	3480	±24
PR-16	15TKPB17	SHRIMP #1	305	68	0.22	0.00	0.761	±1.94	0.34293	±0.23	1.0	3676	±4
PR-17	15TKPB17	SHRIMP #1	206	101	0.49	0.53	0.499	±2.00	0.27530	±0.39	26.6	3336	±6
PR-18	15TKPB17	SHRIMP #1	215	110	0.51	0.03	0.772	±1.99	0.35180	±0.27	0.9	3715	±4
PR-19	15TKPB17	SHRIMP #1	141	58	0.41	0.03	0.776	±2.07	0.35595	±0.33	1.1	3733	±5
PR-20	15TKPB17	SHRIMP #1	713	123	0.17	0.08	0.537	±5.20	0.28661	±3.61	22.7	3399	±56
PR-21	15TKPB17	SHRIMP #1	132	97	0.73		0.735	±2.09	0.32396	±0.68	1.3	3589	±10
PR-22	15TKPB17	SHRIMP #1	496	282	0.57	0.07	0.657	±1.89	0.30520	±0.19	8.8	3497	±3
PR-23	15TKPB17	SHRIMP #1	151	83	0.55	0.11	0.594	±2.07	0.29625	±0.41	16.1	3451	±6
PR-24	15TKPB17	SHRIMP #1	421	237	0.56	0.04	0.595	±1.91	0.27864	±0.27	12.9	3355	±4
PR-25	15TKPB17	SHRIMP #1	366	177	0.48	0.06	0.568	±1.91	0.25172	±0.39	11.6	3196	±6
PR-26	15TKPB17	SHRIMP #1	680	101	0.15	0.13	0.722	±1.87	0.30959	±0.31	0.6	3519	±5
PR-27	15TKPB17	SHRIMP #1	883	239	0.27	0.07	0.546	±1.86	0.25244	±0.40	15.1	3200	±6
15tkpb17-01	15TKPB17	SHRIMP #2	346	161	0.47	0.10	0.559	±1.99	0.32263	±0.17	24.7	3580	±3
15tkpb17-02	15TKPB17	SHRIMP #2	333	103	0.31	0.14	0.712	±1.62	0.35625	±0.15	9.2	3731	±2
15tkpb17-03	15TKPB17	SHRIMP #2	626	556	0.89	0.36	0.550	±1.69	0.27138	±0.13	18.1	3302	±2
15tkpb17-04	15TKPB17	SHRIMP #2	676	159	0.23	0.19	0.634	±1.60	0.32500	±0.12	15.0	3589	±2
15tkpb17-05	15TKPB17	SHRIMP #2	184	87	0.47	0.10	0.671	±1.64	0.29688	±0.23	5.3	3451	±4
15tkpb17-06	15TKPB17	SHRIMP #2	283	152	0.54	0.00	0.692	±1.62	0.29727	±0.18	2.5	3456	±3
15tkpb17-07	15TKPB17	SHRIMP #2	280	170	0.61		0.684	±1.59	0.29427	±0.18	2.9	3440	±3
15tkpb17-08	15TKPB17	SHRIMP #2	185	70	0.38	0.04	0.700	±1.64	0.29652	±0.22	1.2	3451	±3
15tkpb17-09	15TKPB17	SHRIMP #2	269	132	0.49	0.00	0.697	±1.78	0.29778	±0.18	1.8	3459	±3
15tkpb17-10	15TKPB17	SHRIMP #2	694	191	0.28	0.07	0.698	±2.83	0.29025	±1.46	-0.3	3417	±23
15tkpb17-11	15TKPB17	SHRIMP #2	143	71	0.50		0.683	±1.84	0.29571	±0.25	3.4	3449	±4
15tkpb17-12	15TKPB17	SHRIMP #2	152	62	0.41	0.10	0.681	±1.65	0.31958	±0.22	7.8	3565	±3
15tkpb17-13	15TKPB17	SHRIMP #2	129	82	0.64	0.16	0.432	±1.66	0.34482	±0.28	44.0	3681	±5
15tkpb17-14	15TKPB17	SHRIMP #2	80	41	0.51	0.13	0.578	±1.70	0.34661	±0.33	25.3	3689	±5
18appb12-01	18APPB12	SHRIMP #2	250	161	0.65	0.01	0.755	±1.69	0.36244	±0.17	4.6	3760	±3
18appb12-02	18APPB12	SHRIMP #2	207	102	0.49	0.01	0.728	±1.70	0.36068	±0.19	7.9	3753	±3
18appb12-03	18APPB12	SHRIMP #2	410	113	0.28	0.11	0.415	±1.99	0.32805	±0.16	44.7	3605	±3
18appb12-04	18APPB12	SHRIMP #2	438	75	0.17	0.08	0.236	±1.78	0.33553	±0.21	69.0	3641	±3
18appb12-05	18APPB12	SHRIMP #2	189	84	0.45	0.03	0.669	±1.63	0.29507	±0.21	5.3	3444	±3
18appb12-06	18APPB12	SHRIMP #2	155	76	0.49		0.695	±1.65	0.29861	±0.24	2.3	3463	±4
18appb12-07	18APPB12	SHRIMP #2	467	188	0.40	0.06	0.668	±1.96	0.31693	±0.14	9.2	3554	±2
18appb12-08	18APPB12	SHRIMP #2	41	26	0.64		0.708	±1.81	0.29424	±0.45	0.3	3442	±7
18appb12-09	18APPB12	SHRIMP #2	523	336	0.64	0.09	0.594	±2.01	0.29617	±0.14	16.0	3448	±2
18appb12-10	18APPB12	SHRIMP #2	139	59	0.43	0.00	0.692	±1.66	0.29667	±0.25	2.4	3453	±4
18appb12-11	18APPB12	SHRIMP #2	174	51	0.29	0.00	0.687	±1.71	0.29560	±0.22	2.8	3447	±3
18appb13-01	18APPB13	SHRIMP #2	194	75	0.39		0.517	±1.63	0.33186	±0.23	31.6	3626	±4
18appb13-02	18APPB13	SHRIMP #2	158	30	0.19	0.02	0.702	±1.64	0.32442	±0.22	5.8	3590	±3
18appb13-03	18APPB13	SHRIMP #2	476	143	0.30	0.06	0.297	±1.74	0.34367	±0.18	61.4	3678	±3
18appb13-04	18APPB13	SHRIMP #2	120	74	0.61		0.769	±1.82	0.35478	±0.24	1.7	3729	±4
18appb13-05	18APPB13	SHRIMP #2	280	57	0.20	0.04	0.473	±2.73	0.33737	±0.19	37.9	3650	±3
18appb13-06	18APPB13	SHRIMP #2	193	58	0.30		0.743	±1.64	0.32685	±0.21	0.8	3603	±3
18appb13-07	18APPB13	SHRIMP #2	159	115	0.72	0.00	0.780	±1.65	0.35264	±0.21	0.0	3718	±3
18appb13-08	18APPB13	SHRIMP #2	151	66	0.43	0.08	0.403	±1.75	0.34274	±0.25	48.0	3675	±4
18appb13-09	18APPB13	SHRIMP #2	97	31	0.32	0.03	0.567	±1.68	0.32650	±0.32	24.0	3601	±5
18appb16-01	18APPB16	SHRIMP #2	149	65	0.44	0.03	0.643	±2.15	0.34768	±0.22	17.0	3696	±3
18appb16-02	18APPB16	SHRIMP #2	208	193	0.93	0.00	0.745	±1.63	0.32892	±0.19	0.9	3612	±3
18appb16-03	18APPB16	SHRIMP #2	343	154	0.45	0.00	0.697	±1.69	0.29719	±0.16	1.7	3456	±3
18appb16-03b	18APPB16	SHRIMP #2	287	105	0.36		0.676	±1.66	0.29524	±0.18	4.4	3446	±3
n5932_15TKPB17-01a	15TKPB17	Nordsim	457	127	0.28	0.11	0.675	±0.92	0.33494	±0.20	11.0	3640	±3
n5932_15TKPB17-01b	15TKPB17	Nordsim	342	204	0.60	0.23	0.548	±2.25	0.34920	±0.19	29.5	3704	±3
n5932_15TKPB17-02a	15TKPB17	Nordsim	360	44	0.12	0.09	0.708	±1.26	0.33318	±0.50	6.4	3632	±8
n5932_15TKPB17-02b	15TKPB17	Nordsim	241	61	0.25	0.06	0.677	±0.97	0.31074	±0.28	6.9	3525	±4
n5932_15TKPB17-03	15TKPB17	Nordsim	245	139	0.57	0.02	0.777	±1.07	0.35580	±0.19	1.0	3732	±3
n5932_15TKPB17-04a	15TKPB17	Nordsim	411	305	0.74	0.18	0.557	±0.94	0.26410	±0.33	15.7	3271	±5
n5932_15TKPB17-04b	15TKPB17	Nordsim	203	121	0.60	0.01	0.771	±1.10	0.35070	±0.13	0.9	3710	±2
n5932_15TKPB17-05	15TKPB17	Nordsim	311	73	0.24	0.03	0.760	±1.07	0.34826	±0.10	2.0	3699	±1
n5932_15TKPB17-06	15TKPB17	Nordsim	1568	582	0.37	0.32	0.454	±1.13	0.23533	±0.68	26.1	3089	±11
n5932_15TKPB17-07	15TKPB17	Nordsim	10240	15496	1.51	0.93	0.130	±2.07	0.12431	±1.60	64.8	2019	±28
n5932_15TKPB17-08	15TKPB17	Nordsim	28088	74602	2.66	1.58	0.036	±2.44	0.09210	±2.08	86.0	1469	±39
n5932_15TKPB17-09	15TKPB17	Nordsim	882	373	0.42	0.36	0.494	±2.26	0.26361	±1.92	25.2	3268	±30
n5932_15TKPB17-10	15TKPB17	Nordsim	1083	227	0.21	0.32	0.548	±0.88	0.27251	±0.57	18.7	3321	±9
n5932_15TKPB17-11	15TKPB17	Nordsim	10784	11238	1.04	0.80	0.118	±3.72	0.12489	±0.80	68.0	2027	±14
n5932_15TKPB17-12	15TKPB17	Nordsim	10525	8127	0.77	0.81	0.169	±1.64	0.12813	±1.58	55.3	2072	±28
n5932_15TKPB17-13	15TKPB17	Nordsim	1408	698	0.50	0.42	0.314	±1.28	0.23066	±0.51	48.3	3057	±8
n5932_15TKPB17-14	15TKPB17	Nordsim	210	34	0.16	0.02	0.751	±1.55	0.35134	±0.34	3.6	3713	±5
n5932_15TKPB17-15a	15TKPB17	Nordsim	235	136	0.58	0.02	0.774	±1.12	0.35501	±0.11	1.2	3729	±2
n5932_15TKPB17-15b	15TKPB17	Nordsim	253	146	0.58	0.00	0.775	±1.14	0.35654	±0.10	1.2	3735	±2
n5932_15TKPB17-16	15TKPB17	Nordsim	377	309	0.82	0.19	0.424	±1.97	0.31477	±0.29	42.1	3544	±5
n5932_15TKPB17-17	15TKPB17	Nordsim	142	68	0.48	0.03	0.693	±1.23	0.29743	±0.16	2.4	3457	±3
n5932_15TKPB17-18	15TKPB17	Nordsim	7031	2009	0.29	0.58	0.236	±1.46	0.14195	±1.24	43.6	2251	±21
n5932_15TKPB17-19	15TKPB17	Nordsim	189	57	0.30	0.01	0.698	±1.02	0.29651	±0.16	1.5	3452	±3
n5932_15TKPB17-20	15TKPB17	Nordsim	970	636	0.66	0.21	0.580	±1.07	0.27259	±0.10	13.9	3321	±2
n5932_15TKPB17-21	15TKPB17	Nordsim	474	336	0.71	0.09	0.679	±1.14	0.30459	±0.11	5.6	3494	±2
n5932_15TKPB17-22	15TKPB17	Nordsim	249	189	0.76	9.76	0.408	±24.65	0.22882	±16.64	32.4	3044	±270
n5932_15TKPB17-23	15TKPB17	Nordsim	347	196	0.57	0.10	0.584	±1.11	0.29024	±0.16	16.5	3419	±3
n5932_15TKPB17-24	15TKPB17	Nordsim	728	662	0.91	0.41	0.350	±1.45	0.20647	±4.44	37.9	2878	±72
n5932_15TKPB17-25	15TKPB17	Nordsim	292	143	0.49	0.09	0.664	±0.97	0.28834	±0.13	4.7	3409	±2
n5932_15TKPB17-26	15TKPB17	Nordsim	407	267	0.66	0.21	0.599	±1.45	0.26798	±0.12	10.3	3294	±2
n5932_15TKPB17-27	15TKPB17	Nordsim	601	219	0.36	0.12	0.690	±1.95	0.30875	±0.49	4.9	3515	±8
n5932_15TKPB17-28	15TKPB17	Nordsim	247	126	0.51	0.01	0.687	±1.03	0.29570	±0.12	2.9	3448	±2
n5932_15TKPB17-29	15TKPB17	Nordsim	526	428	0.81	0.86	0.320	±2.62	0.27245	±1.22	52.5	3320	±19
n5932_15TKPB17-30	15TKPB17	Nordsim	195	102	0.52	0.12	0.553	±1.85	0.29577	±0.23	21.8	3448	±3
n5932_15TKPB17-31	15TKPB17	Nordsim	716	323	0.45	0.18	0.589	±1.02	0.27330	±0.23	12.7	3325	±4
n5932_15TKPB17-32	15TKPB17	Nordsim	293	167	0.57	0.13	0.676	±1.37	0.28958	±0.42	3.2	3415	±7
n5932_15TKPB17-33	15TKPB17	Nordsim	1695	685	0.40	0.37	0.442	±0.97	0.23231	±0.47	27.5	3068	±8
n5932_15TKPB17-34	15TKPB17	Nordsim	311	207	0.66	0.18	0.561	±1.17	0.25777	±0.70	13.9	3233	±11
n5932_15TKPB17-35	15TKPB17	Nordsim	161	75	0.47	0.01	0.701	±1.86	0.29635	±0.35	1.1	3451	±5
n5932_15TKPB17-36	15TKPB17	Nordsim	1994	2563	1.29	0.54	0.384	±4.46	0.20795	±1.61	32.1	2890	±26
n5932_15TKPB17-37	15TKPB17	Nordsim	6077	1012	0.17	2.21	0.333	±2.53	0.15755	±0.63	27.2	2430	±11
n5932_15TKPB17-38	15TKPB17	Nordsim	771	418	0.54	0.17	0.594	±2.37	0.26879	±1.76	11.0	3299	±28
n5932_15TKPB17-39	15TKPB17	Nordsim	480	51	0.11	0.02	0.716	±1.02	0.31915	±0.30	3.1	3566	±5
n5932_15TKPB17-40	15TKPB17	Nordsim	956	740	0.77	0.41	0.466	±3.63	0.23596	±3.51	24.4	3093	±56
n5932_15TKPB17-41	15TKPB17	Nordsim	69	36	0.53	0.03	0.777	±1.14	0.35916	±0.21	1.4	3746	±3
n5932_15TKPB17-42	15TKPB17	Nordsim	1230	903	0.73	0.28	0.353	±0.97	0.26299	±0.45	46.4	3265	±7
n5932_15TKPB17-43	15TKPB17	Nordsim	1047	643	0.61	0.26	0.575	±0.80	0.26159	±0.31	12.5	3256	±5

* Letter b denotes second analyses on the same zircon grain

† % of common ^{206}Pb in measured ^{206}Pb, estimated from ^{204}Pb assuming a present day Stacey and Kramers (1975) model for terrestrial Pb-isotope composition.

§ Age discordance in conventional concordia space. Negative numbers are reverse discordant.

Table A2. Major and Trace element data

Sample	15TKPB17	18APPB16	Kerba monzogranite	KG1*	Bunbury Basalt (BB1)	BB1*
Major elements						
SiO_2	82.1	84.3	71.50	71.37	52.20	51.82
TiO_2	0.14	0.17	0.24	0.24	2.04	2.02
Al_2O_3	10.4	12.6	15.00	14.95	15.40	15.33
Fe_2O_3	0.2	0.1	0.72	0.65	3.55	3.28
FeO	0.0	0.0	1.19	1.29	7.78	7.99
FeO^{tot}	0.24	0.07				
MgO	0.74	0.02	0.04	0.04	0.16	0.16
MnO	n/a	n/a	0.48	0.48	4.63	4.72
CaO	0.69	0.00	2.14	2.16	8.66	8.71
Na_2O	0.07	0.09	4.2	4.07	3.09	3.03
K_2O	2.99	0.293	3.48	3.47	0.45	0.46
P_2O_5	0.013	0.025	0.064	0.08	0.242	0.25
SO_3	0.02	n/a	0.015	0.03	0.154	0.16
BaO	0.113	0.0475	0.166	0.0137	0.017	0.015
LOI_{tot}	2.6	2.32	0.5		0.34	
Total	100.1	99.9	99.73		98.71	
Trace elements						
Ba	113	47.5	1420	1373	168	152
Rb	62.2	7.1	90.5	96	12.1	12.4
Sr	24.7	31.5	564	515	273	245
Zr	105	122	175	190	154	153
Nb	2.9	3.38	8.68	9.5	6.87	7.6
Y	3.82	4.88	4.66	4.5	41.9	39.8
Sc	3.1	n/a	1.4	2.4	26.7	27.7
V	12.5	9.6	14	14.6	248	245
Cr	2	n/a	161	170	146	150
Co	19.9	23.4	2.8	-	36.3	37
Ni	4	4	6	8	54	41
Cu	n/a	n/a	4	6.2	80	82
Zn	n/a	n/a	50	41	130	116
Ga	15.9	17.8	18.4	20	23.5	23
La	24.4	31.9	43.9	43.8	11.6	10.95
Ce	41.3	55.1	69.2	71.3	27.9	26.8
Pr	4.36	5.98	7.1	6.6	4.1	3.6
Nd	14.7	19.6	21.9	22.4	19.9	18.75
Sm	2.1	3.28	3.25	2.8	6.06	5.69
Eu	0.45	0.84	0.73	0.8	1.94	2.01
Gd	1.16	1.9	1.63	1.5	7.29	7.26
Tb	0.16	0.2	0.18	0.2	1.21	1.22
Dy	0.81	1.19	0.78	0.8	7.27	7.27
Ho	0.15	0.19	0.15	0.1	1.51	1.46
Er	0.37	0.38	0.4	0.4	4.04	3.95
Tm	0.05	0.08	0.07	-	0.56	0.53
Yb	0.39	0.4	0.44	0.5	3.36	3.32
Lu	0.06	0.08	0.08	0.1	0.48	0.49
Hf	2.83	3.44	4.62	5	4.04	4
Ta	0.4	0.52	0.93	1	0.44	0.5
Pb	5	3	38	40	4	4
Th	7.84	10.6	15.8	17.4	1.63	1.8
U	2.04	1.78	3.74	4.2	0.29	0.3

Note: Majors have been determined by X-Ray Fluorescence Spectrometry.
Traces have been determined by Laser Ablation Inductively Coupled Plasma Mass Spectrometry.
Loss on Ignition results have been determined using a robotic TGA system at 1000°C.
Ferrous Iron (FeO) content was determined by acid digestion followed by volumetric titration.
$FeO^{tot}=FeO+0.8998*Fe_2O_3$
*Suggested reference-values for the Kerba monzogranite and the Bunbury Basalt from, Morris (2007).

Table A3. Zircon O-isotopes

Spot I.D	Corresponding U–Pb spot I.D	Comment	Sequential no.*	Drift, back-ground and SIMS corrected	abs.	$\delta^{18}O^{\S}$	abs.	Field aperture		Mount location		$^{207}Pb^{d}$		Th/U#	Disc. %#,**
				$^{18}O/^{16}O^{\dagger}$	1s	(‰)	2s	X	Y	X-pos.	Y-pos.	^{206}Pb	1s		
Cameca IMS 1280 multi-collector ion microprobe Centre for Microscopy, Characterisation and Analysis, University of Western Australia.															
Session I															
15TKPB17	**Corresp. U–Pb**														
15TKPB17-01	15tkpb17-03	*Small crack*	*7*	*0.0020128*	*±0.00000046*	*3.78*	*±0.45*	*-11*	*13*	*2425*	*3083*	3302	±2	0.89	18.1
15TKPB17-02	15tkpb17-09	ok	8	0.0020167	±0.00000047	5.71	±0.47	-12	12	2182	2994	3459	±3	0.49	1.8
15TKPB17-03	15tkpb17-08	ok	9	0.0020160	±0.00000048	5.39	±0.48	-11	13	2719	3100	3451	±3	0.38	1.2
15TKPB17-04	15tkpb17-02	ok	10	0.0020151	±0.00000050	4.94	±0.50	-8	11	3851	3022	3731	±2	0.31	9.2
15TKPB17-04b	15tkpb17-02	ok	11	0.0020164	±0.00000046	5.59	±0.46	-8	10	3871	3009	3731	±2	0.31	9.2
15TKPB17-05	15tkpb17-07	ok	16	0.0020166	±0.00000050	5.69	±0.50	-7	9	4590	2865	3440	±3	0.61	2.9
15TKPB17-06	15tkpb17-01	*Crack*	*17*	*0.0020151*	*±0.00000050*	*4.92*	*±0.50*	*-7*	*8*	*4721*	*2718*	3580	±3	0.47	24.7
15TKPB17-06b	15tkpb17-01	*Crack*	*18*	*0.0020140*	*±0.00000045*	*4.40*	*±0.45*	*-8*	*9*	*4696*	*2695*	3580	±3	0.47	24.7
15TKPB17-06c	15tkpb17-01	ok	19	0.0020160	±0.00000046	5.37	±0.46	-8	8	4676	2712	3580	±3	0.47	24.7
15TKPB17-07		ok	20	0.0020160	±0.00000057	5.40	±0.57	-7	8	5268	2605				
15TKPB17-08	15tkpb17-05	ok	23	0.0020168	±0.00000040	5.79	±0.40	-5	7	5793	2525	3451	±4	0.47	5.3
15TKPB17-09	15tkpb17-04	*Metamict zone*	*24*	*0.0020130*	*±0.00000046*	*3.88*	*±0.46*	*-14*	*8*	*1803*	*1627*	3589	±2	0.23	15.0
15TKPB17-09b	15tkpb17-04	*Metamict zone*	*25*	*0.0020140*	*±0.00000046*	*4.38*	*±0.46*	*-14*	*8*	*1840*	*1629*	3589	±2	0.23	15.0
15TKPB17-10		ok	26	0.0020173	±0.00000043	6.05	±0.43	-9	4	4825	1125				
15TKPB17-11		ok	27	0.0020179	±0.00000046	6.33	±0.46	-9	4	4665	1094				
15TKPB17-12		ok	28	0.0020158	±0.00000053	5.30	±0.53	-17	9	233	2257				
15TKPB17-13		ok	33	0.0020171	±0.00000045	5.93	±0.45	-17	10	226	2337				
15TKPB17-14		ok	34	0.0020163	±0.00000043	5.55	±0.43	-17	9	-290	2037				
15TKPB17-15		ok	35	0.0020167	±0.00000053	5.73	±0.53	-17	10	656	2115				
15TKPB17-15b		ok	36	0.0020175	±0.00000050	6.13	±0.50	-17	10	654	2099				
15TKPB17-16		ok	37	0.0020171	±0.00000049	5.92	±0.49	-16	7	735	1756				
Weighted average						**5.70**	**±0.25**	**n=16**	**MSDW=0.54**						
18APPB12															
18APPB12-01	18appb12-01	ok	117	0.0020160	±0.00000053	5.36	±0.53	-15	1	-144	-822	3760	±3	0.65	4.6
18APPB12-01b	18appb12-01	ok	118	0.0020161	±0.00000047	5.42	±0.47	-14	1	-106	-831	3760	±3	0.65	4.6
18APPB12-02	18appb12-02	*Crack*	*121*	*0.0020144*	*±0.00000058*	*4.57*	*±0.57*	*-14*	*0*	*-14*	*-977*	3753	±3	0.49	7.9
18APPB12-02b	18appb12-02	*Crack*	*122*	*0.0020124*	*±0.00000042*	*3.57*	*±0.42*	*-14*	*0*	*-6*	*-967*	3753	±3	0.49	7.9
18APPB12-03	18appb12-10	*Crack*	*123*	*0.0020174*	*±0.00000055*	*6.08*	*±0.55*	*-14*	*0*	*114*	*-1100*	3453	±4	0.43	2.4
18APPB12-04		ok	124	0.0020168	±0.00000048	5.79	±0.48	-14	2	474	-862				
18APPB12-05	18appb12-08	ok	125	0.0020174	±0.00000043	6.10	±0.43	-12	0	1053	-1199	3442	±7	0.64	-0.3
18APPB12-05b	18appb12-08	ok	126	0.0020182	±0.00000042	6.47	±0.42	-12	-1	1038	-1172	3442	±7	0.64	-0.3
18APPB12-06	18appb12-06	ok	127	0.0020184	±0.00000047	6.57	±0.47	-15	-2	3280	-1255	3463	±4	0.49	2.3
18APPB12-07	18appb12-03	ok	131	0.0020178	±0.00000059	6.27	±0.59	-5	-1	4554	-1360	3605	±3	0.28	44.7
18APPB12-08		ok	132	0.0020173	±0.00000056	6.05	±0.56	-5	-2	4356	-1493				
18APPB12-09	18appb12-04	ok	133	0.0020159	±0.00000052	5.31	±0.52	-4	-1	4972	-1520	3641	±3	0.17	69.0
18APPB12-10	18appb12-05	ok	134	0.0020172	±0.00000051	5.97	±0.50	-4	-1	4887	-1513	3444	±3	0.45	5.3
18APPB12-10b	18appb12-05	ok	135	0.0020168	±0.00000051	5.80	±0.51	-4	-1	4920	-1491	3444	±3	0.45	5.3
18APPB12-11	18appb12-11	ok	136	0.0020172	±0.00000051	6.00	±0.51	-14	-2	-71	-2498	3447	±3	0.29	2.8
Weighted average						**5.95**	**±0.31**	**n=12**	**MSDW=0.72**						
18APPB13															
18APPB13-01		ok	41	0.0020190	±0.00000047	6.87	±0.47	-16	5	-3258	270				
18APPB13-02		ok	42	0.0020173	±0.00000054	6.03	±0.54	-15	5	-3198	191				
18APPB13-03	18appb13-06	ok	43	0.0020164	±0.00000047	5.57	±0.46	-17	6	-3326	195	3603	±3	0.30	0.8
18APPB13-03b	18appb13-06	ok	44	0.0020158	±0.00000047	5.29	±0.47	-16	6	-3340	186	3603	±3	0.30	0.8
18APPB13-04	18appb13-07	ok	45	0.0020157	±0.00000048	5.24	±0.48	-14	4	-3286	-235	3718	±3	0.72	0.0
18APPB13-04b	18appb13-07	ok	46	0.0020148	±0.00000048	4.78	±0.48	-16	6	-3248	-233	3718	±3	0.72	0.0
18APPB13-05		ok	51	0.0020177	±0.00000050	6.24	±0.49	-15	4	-3418	-327				
18APPB13-06		ok	52	0.0020161	±0.00000047	5.42	±0.47	-15	5	-3532	-149				
18APPB13-07	18appb13-08	*Big crack*	*53*	*0.0020213*	*±0.00000044*	*8.02*	*±0.44*	*-15*	*3*	*-3605*	*-163*	3675	±4	0.43	48.0
18APPB13-07b	18appb13-08	ok	54	0.0020134	±0.00000051	4.11	±0.50	-14	4	-3607	-183	3675	±4	0.43	48.0
18APPB13-08	18appb13-09	ok	55	0.0020166	±0.00000045	5.69	±0.45	-15	3	-3175	-560	3601	±5	0.32	24.0
18APPB13-09	18appb13-05	ok	59	0.0020163	±0.00000049	5.52	±0.49	-14	3	-3522	-539	3650	±3	0.20	37.9
18APPB13-10	18appb13-04	*Crack*	*60*	*0.0020149*	*±0.00000040*	*4.84*	*±0.40*	*-14*	*4*	*-3531*	*-641*	3729	±4	0.61	1.7
18APPB13-10b	18appb13-04	ok	61	0.0020160	±0.00000045	5.36	±0.45	-15	4	-3520	-674	3729	±4	0.61	1.7
18APPB13-11		ok	62	0.0020164	±0.00000048	5.57	±0.48	-15	2	-3305	-912				
18APPB13-12		*Crack*	*63*	*0.0020253*	*±0.00000047*	*10.01*	*±0.47*	*-15*	*1*	*-3239*	*-1200*				
18APPB13-13		ok	64	0.0020173	±0.00000049	6.02	±0.49	-14	1	-3369	-1380				
18APPB13-14	18appb13-03	ok	68	0.0020180	±0.00000049	6.39	±0.48	-14	1	-3780	-1379	3678	±3	0.30	61.4
18APPB13-15		ok	69	0.0020183	±0.00000052	6.51	±0.52	-20	1	-3308	-1882				
18APPB13-15b		ok	70	0.0020179	±0.00000051	6.35	±0.51	-19	0	-3355	-1870				
18APPB13-16		*Crack*	*71*	*0.0020195*	*±0.00000054*	*7.15*	*±0.54*	*-28*	*2*	*-3410*	*-2288*				
18APPB13-17		ok	72	0.0020172	±0.00000050	5.99	±0.50	-33	2	-3504	-2388				
18APPB13-04	18appb13-02	ok	73	0.0020156	±0.00000045	5.20	±0.45	-34	2	-3453	-2517	3590	±3	0.19	5.8
18APPB13-05		ok	77	0.0020156	±0.00000048	5.18	±0.47	-32	-1	-3328	-2830				
18APPB13-04		ok	78	0.0020171	±0.00000056	5.94	±0.56	-32	-3	-3292	-2834				
Weighted average						**5.73**	**±0.23**	**n=21**	**MSDW=1.25**						
18APPB16															
18APPB16-01	18appb16-01	ok	88	0.0020166	±0.00000045	5.68	±0.45	-19	-5	-2151	-2688	3696	±3	0.44	17.0
18APPB16-01b	18appb16-01	*Big crack*	*89*	*0.0020222*	*±0.00000050*	*8.48*	*±0.50*	*-19*	*-5*	*-2152*	*-2720*	3696	±3	0.44	17.0
18APPB16-02		ok	90	0.0020172	±0.00000045	5.97	±0.45	-19	-4	-2187	-2613				
18APPB16-03		ok	91	0.0020179	±0.00000050	6.32	±0.50	-18	-3	-2500	-2603				
18APPB16-05		*Big crack*	*96*	*0.0020202*	*±0.00000048*	*7.46*	*±0.48*	*-31*	*-3*	*-2525*	*-2900*				
18APPB16-05b		*Crack*	*97*	*0.0020177*	*±0.00000053*	*6.23*	*±0.53*	*-32*	*-2*	*-2528*	*-2922*				
18APPB16-06	18appb16-02	ok	98	0.0020177	±0.00000043	6.22	±0.43	-15	-2	-2498	-2130	3612	±3	0.93	0.9
18APPB16-07		ok	99	0.0020163	±0.00000043	5.56	±0.43	-15	-1	-2493	-1981				
18APPB16-08	18appb16-03	ok	100	0.0020180	±0.00000049	6.37	±0.49	-17	-3	-1617	-2236	3456	±3	0.45	1.7
18APPB16-08b	18appb16-03	ok	104	0.0020175	±0.00000047	6.11	±0.47	-15	-3	-1621	-2252	3456	±3	0.45	1.7
18APPB16-09		ok	105	0.0020168	±0.00000050	5.79	±0.50	-16	2	-1483	-633				
18APPB16-10		ok	106	0.0020169	±0.00000052	5.84	±0.52	-16	3	-1623	-519				
18APPB16-10b		ok	107	0.0020169	±0.00000049	5.85	±0.49	-17	3	-1605	-486				
18APPB16-11		ok	108	0.0020176	±0.00000046	6.18	±0.46	-16	3	-1477	-390				
18APPB16-12		ok	109	0.0020170	±0.00000051	5.86	±0.51	-16	4	-1635	-101				
18APPB16-12b		ok	113	0.0020169	±0.00000049	5.82	±0.49	-16	4	-1605	-104				
18APPB16-13		ok	114	0.0020173	±0.00000053	6.02	±0.53	-15	7	-2668	760				
18APPB16-13b		ok	115	0.0020173	±0.00000054	6.03	±0.54	-15	7	-2628	764				
18APPB16-14		ok	116	0.0020168	±0.00000050	5.77	±0.50	-16	9	-1356	1627				
Weighted average						**5.96**	**±0.26**	**n=16**	**MSDW=0.25**						

Session II

15TKPB17

15TKPB17-01	n5932_15TKPB17-17	*Crack*	*8*	*0.0020179*	*±0.00000030*	*6.35*	*±0.30*	*10*	*20*	*532*	*980*	3457	±3	0.48	2.4
15TKPB17-02	PR-5	ok	9	0.0020167	±0.00000029	5.72	±0.29	11	20	314	1024	3746	±4	0.36	0.0
15TKPB17-03	n5932_15TKPB17-01t	ok	10	0.0020173	±0.00000030	6.04	±0.30	11	19	153	1693	3704	±3	0.60	29.5
15TKPB17-04	n5932_15TKPB17-30	ok	11	0.0020178	±0.00000032	6.28	±0.32	11	19	-749	1450	3448	±3	0.52	21.8
15TKPB17-05	n5932_15TKPB17-28	ok	16	0.0020176	±0.00000032	6.17	±0.32	11	20	-480	2457	3448	±2	0.51	2.9
15TKPB17-06	n5932_15TKPB17-03	ok	17	0.0020157	±0.00000030	5.24	±0.29	11	19	760	2112	3732	±3	0.57	1.0
15TKPB17-06b	n5932_15TKPB17-03	ok	18	0.0020158	±0.00000032	5.29	±0.32	11	19	766	2165	3732	±3	0.57	1.0
15TKPB17-07	n5932_15TKPB17-19	ok	19	0.0020163	±0.00000034	5.56	±0.34	12	19	1081	1925	3452	±3	0.31	1.5
15TKPB17-08	PR-18	ok	20	0.0020177	±0.00000032	6.21	±0.32	13	19	1039	2508	3715	±4	0.51	0.9
15TKPB17-09	n5932_15TKPB17-41	*Inclusion*	*24*	*0.0020122*	*±0.00000028*	*3.50*	*±0.28*	*12*	*19*	*447*	*3131*	3746	±3	0.53	1.4
15TKPB17-09b	n5932_15TKPB17-41	*Crack*	*25*	*0.0020138*	*±0.00000030*	*4.26*	*±0.30*	*12*	*19*	*426*	*3154*	3746	±3	0.53	1.4
15TKPB17-10	n5932_15TKPB17-02t	ok	26	0.0020173	±0.00000031	6.04	±0.31	12	17	1224	1588	3525	±4	0.26	6.9
15TKPB17-11	n5932_15TKPB17-15c	ok	27	0.0020154	±0.00000030	5.11	±0.30	10	20	1361	1226	3729	±2	0.59	1.2
15TKPB17-11b	n5932_15TKPB17-15t	ok	28	0.0020157	±0.00000031	5.26	±0.31	10	20	1387	1212	3735	±2	0.58	1.2
15TKPB17-11c	n5932_15TKPB17-15t	ok	34	0.0020154	±0.00000031	5.06	±0.30	9	20	1370	1166	3735	±2	0.58	1.2
15TKPB17-11d	n5932_15TKPB17-15t	ok	35	0.0020157	±0.00000032	5.22	±0.32	9	19	1368	1113	3735	±2	0.58	1.2
15TKPB17-12	n5932_15TKPB17-35	*Crack*	*33*	*0.0020136*	*±0.00000031*	*4.20*	*±0.31*	*10*	*19*	*1386*	*1205*	3451	±5	0.47	1.1
15TKPB17-12b	n5932_15TKPB17-35	ok	37	0.0020174	±0.00000030	6.07	±0.29	8	20	1641	501	3451	±5	0.47	1.1
15TKPB17-13	PR-03	ok	36	0.0020174	±0.00000032	6.09	±0.32	9	19	1636	559	3457	±6	0.48	3.2
Weighted average		**15TKPB17 Session II**				**5.68**	**±0.17**	**n=15**	**MSDW=2.18**						
Weighted average		**15TKPB17 Session I & II combined**				**5.69**	**±0.14**	**n=31**	**MSDW=1.29**						
Weighted average		**All analyses both sessions**				**5.75**	**±0.10**	**n=31**	**MSDW=1.15**						

Note: Each $\delta^{18}O$ error (2σ) represents the counting statistics errors for each individual spot and the external error based on all standards analysed during the session, which were added in quadrature.

Field aperture centering digits are given and show little difference between standard and sample. mount. The location of the unknowns is proximal.

Mount position X Y for standard and sample indicates that most analyses are within the central region to standards.

Values in italic are interpreted to be unreliable due to sampling of discordant grains, inclusions, mixed domains, or on fractures.

Italic denotes discarded analyses.

If mutliple U–Pb analyses on one grain, data from the nearest analyses is denoted in $^{207}Pb/^{207}Pb$, Th/U and Discordance columns.

*Sequential order of analyses.

†Raw ratios drift corrected using the standard analyses versus time. The instrumental mass fractionation, corrected using alpha SIMS (ratio between the session average standard value and reference v

§Normalised to a $\delta^{18}O$ value of 9.20‰ for the Temora 2 standard.

#When multiple analyses on single grain, $^{207}Pb/^{206}Pb$-date, Th/U and discordance of U–Pb of analysis closest to O-isotope sopt is denoted.

**Age discordance in conventional concordia space. Negative numbers are reverse discordant

Table A4. Standrad zircon O-isotopes

Spot I.D	Sequential no.*	Drift, background and SIMS corrected	abs.	$\delta^{18}O^{\S}$	abs.	Field aperture		Mount location	
		$^{18}O/^{16}O$†	1σ	(‰)	2σ	X	Y	X-pos.	Y-pos.
Cameca IMS 1280 multi-collector ion microprobe Centre for Microscopy, Characterisation and Analysis, UWA, Perth.									
Session I									
91500									
91500-01	1	0.0020251	±0.0000005	9.93	±0.48	-8	8	2912	836
91500-02	2	0.0020246	±0.0000005	9.66	±0.47	-9	7	2952	836
91500-03	3	0.0020249	±0.0000005	9.80	±0.50	-10	7	2898	796
91500-04	4	0.0020247	±0.0000005	9.74	±0.47	-10	6	2938	796
91500-05	5	0.0020253	±0.0000005	10.01	±0.47	-9	7	2938	756
91500-07	13	0.0020247	±0.0000005	9.73	±0.52	-11	6	2892	610
91500-09	21	0.0020252	±0.0000005	9.99	±0.49	-11	5	2971	474
91500-10	29	0.0020249	±0.0000005	9.85	±0.53	-11	5	3044	485
91500-11	30	0.0020249	±0.0000004	9.82	±0.44	-11	5	3062	445
91500-12	38	0.0020243	±0.0000005	9.53	±0.47	-11	4	3020	445
91500-13	39	0.0020247	±0.0000005	9.72	±0.46	-11	4	2970	445
91500-14	47	0.0020243	±0.0000005	9.54	±0.45	-11	5	2965	405
91500-15	48	0.0020254	±0.0000005	10.09	±0.46	-11	5	3018	405
91500-16	56	0.0020242	±0.0000004	9.48	±0.45	-11	5	3061	405
91500-17	57	0.0020251	±0.0000005	9.94	±0.45	-11	5	3064	365
91500-18	65	0.0020247	±0.0000005	9.72	±0.50	-11	4	3024	365
91500-19	66	0.0020248	±0.0000005	9.77	±0.48	-11	4	2984	365
91500-20	74	0.0020256	±0.0000005	10.15	±0.46	-12	3	2998	222
91500-21	75	0.0020253	±0.0000005	10.02	±0.52	-11	3	3038	236
91500-22	83	0.0020254	±0.0000005	10.07	±0.53	-12	3	3071	230
91500-23	84	0.0020246	±0.0000004	9.69	±0.44	-12	4	3108	229
91500-24	92	0.0020253	±0.0000005	10.00	±0.46	-11	3	3061	110
91500-25	93	0.0020253	±0.0000004	10.00	±0.44	-11	3	3061	70
91500-26	101	0.0020253	±0.0000005	10.02	±0.54	-10	3	3072	30
91500-27	102	0.0020256	±0.0000005	10.15	±0.46	-10	4	3182	362
91500-28	110	0.0020250	±0.0000004	9.85	±0.44	-10	4	3219	346
91500-29	111	0.0020254	±0.0000005	10.09	±0.46	-9	4	3281	340
91500-30	119	0.0020252	±0.0000005	9.99	±0.47	-10	3	3317	321
91500-31	120	0.0020249	±0.0000005	9.80	±0.52	-9	5	3464	660
91500-32	128	0.0020245	±0.0000005	9.64	±0.53	-9	5	3457	620
91500-33	129	0.0020251	±0.0000005	9.91	±0.50	-9	5	3443	580
91500-34	137	0.0020247	±0.0000005	9.73	±0.50	-10	5	3429	540
91500-35	138	0.0020250	±0.0000005	9.88	±0.48	-10	3	3469	543
91500-36	140	0.0020250	±0.0000005	9.87	±0.55	-11	4	3488	583
91500-37	141	0.0020254	±0.0000005	10.08	±0.50	-11	4	3491	623
91500-38	143	0.0020254	±0.0000005	10.07	±0.54	-11	4	3462	434
91500-39	144	0.0020245	±0.0000005	9.63	±0.54	-11	4	3459	394
91500-40	146	0.0020251	±0.0000006	9.93	±0.58	-10	3	3420	394
91500-41	147	0.0020245	±0.0000006	9.65	±0.56	-10	4	3456	353
		Weighted mean	**2σ**	**Weighted mean**	**2σ**				
91500	**n=39**	**0.0020250**	**±0.0000002**	**9.86**	**±0.16**				
91500 ref		**0.0020250**	**±0.0000002**	**9.86**	**±0.22**				
OGC									
OGC-01	6	0.0020180	±0.0000005	6.37	±0.50	-14	5	1042	914
OGC-02	14	0.0020175	±0.0000005	6.15	±0.50	-15	5	1006	891
OGC-03	22	0.0020169	±0.0000005	5.84	±0.46	-16	5	933	879
OGC-04	31	0.0020174	±0.0000005	6.06	±0.47	-16	5	893	867
OGC-05	40	0.0020170	±0.0000005	5.88	±0.48	-15	6	564	920
OGC-06	49	0.0020169	±0.0000005	5.82	±0.46	-15	5	530	916
OGC-07	58	0.0020171	±0.0000004	5.94	±0.43	-16	5	575	766
OGC-08	76	0.0020170	±0.0000005	5.89	±0.49	-16	5	538	804
OGC-09	94	0.0020158	±0.0000005	5.27	±0.53	-18	5	918	550
OGC-10	112	0.0020167	±0.0000004	5.73	±0.43	-13	6	1045	480
OGC-11	139	0.0020171	±0.0000005	5.92	±0.48	-13	5	1181	608
OGC-12	145	0.0020173	±0.0000005	6.06	±0.48	-11	6	1119	576
		Weighted mean	**2σ**	**Weighted mean**	**2σ**				
OGC	**n=12**	**0.0020170**	**±0.0000003**	**5.91**	**±0.30**				
OGC ref.		**0.0020170**	**±0.0000001**	**5.88**	**±0.06**				
Penglai									
Penglai-01	15	0.0020149	±0.0000004	4.85	±0.43	-13	6	2204	607
Penglai-02	32	0.0020155	±0.0000005	5.12	±0.48	-13	5	2167	618
Penglai-03	50	0.0020150	±0.0000005	4.90	±0.52	-13	5	2118	622
Penglai-04	67	0.0020153	±0.0000005	5.05	±0.48	-13	5	2078	626
Penglai-05	85	0.0020160	±0.0000005	5.40	±0.48	-14	5	2046	602
Penglai-06	103	0.0020153	±0.0000006	5.06	±0.57	-13	4	2243	372
Penglai-07	142	0.0020150	±0.0000005	4.88	±0.53	-13	4	2114	372
Penglai-08	130	0.0020150	±0.0000005	4.89	±0.51	-13	4	2195	383
		Weighted mean	**2σ**	**Weighted mean**	**2σ**				
Penglai		**0.0020152**	**±0.0000004**	**5.02**	**±0.41**				
Penglai ref.		**0.0020158**	**±0.0000001**	**5.31**	**±0.10**				

Session II

Penglai

Penglai-01	1	0.0020159	±0.0000003	5.34	±0.29	21	22	2003	3456
Penglai-02	2	0.0020156	±0.0000003	5.21	±0.31	21	21	2109	3515
Penglai-03	3	0.0020156	±0.0000003	5.19	±0.29	19	21	2076	3436
Penglai-04	4	0.0020162	±0.0000003	5.49	±0.30	20	20	2146	3432
Penglai-05	5	0.0020160	±0.0000003	5.38	±0.30	19	20	2146	3392
Penglai-06	12	0.0020160	±0.0000003	5.40	±0.28	17	19	2146	3352
Penglai-07	13	0.0020159	±0.0000003	5.32	±0.32	17	19	2186	3352
Penglai-08	21	0.0020156	±0.0000003	5.21	±0.29	16	19	2146	3312
Penglai-09	22	0.0020155	±0.0000003	5.14	±0.30	16	19	2186	3312
Penglai-10	29	0.0020156	±0.0000003	5.19	±0.32	16	19	2166	3272
Penglai-11	30	0.0020163	±0.0000003	5.52	±0.32	17	17	2631	3424
Penglai-12	38	0.0020158	±0.0000003	5.28	±0.32	17	17	2671	3433
Penglai-13	39	0.0020157	±0.0000003	5.24	±0.29	16	18	2990	3021
Penglai-14	43	0.0020163	±0.0000003	5.51	±0.33	16	18	2946	2975
Penglai-15	44	0.0020157	±0.0000003	5.23	±0.32	16	18	2986	2975
		Weighted mean	**2σ**	**Weighted mean**	**2σ**				
Penglai		**0.0020158**	**±0.0000002**	**5.31**	**±0.17**				
Penglai ref.		**0.0020158**	**±0.0000001**	**5.31**	**±0.10**				

M257

M257-01	7	0.0020343	±0.0000003	14.51	±0.29	9	18	-2194	2002
M257-02	15	0.0020339	±0.0000003	14.34	±0.33	8	17	-2220	1964
M257-03	31	0.0020341	±0.0000003	14.40	±0.33	7	17	-2234	1779
M257-04	41	0.0020335	±0.0000003	14.10	±0.31	7	18	-2205	1728
M257-05	42	0.0020336	±0.0000003	14.15	±0.29	8	18	-2173	1694
		Weighted mean	**2σ**	**Weighted mean**	**2σ**				
M257 n=5		**0.0020339**	**±0.0000004**	**14.30**	**±0.38**				
M257 ref.		**0.0020331**	**±0.0000002**	**13.93**	**±0.22**				

OGC

OGC-@01	6	0.0020173	±0.0000003	6.04	±0.31	9	20	-307	-1122
OGC-@02	14	0.0020176	±0.0000003	6.20	±0.33	8	19	-348	-1117
OGC-@03	23	0.0020180	±0.0000003	6.38	±0.29	7	19	-381	-1114
OGC-@04	32	0.0020177	±0.0000003	6.24	±0.31	7	20	-290	-1261
OGC-@05	40	0.0020170	±0.0000003	5.87	±0.32	5	20	-285	-1304
OGC-@06	45	0.0020176	±0.0000003	6.21	±0.29	7	20	-609	-1081
		Weighted mean	**2σ**	**Weighted mean**	**2σ**				
OGC n=6		**0.0020175**	**±0.0000003**	**6.17**	**±0.32**				
OGC ref.		**0.0020170**	**±0.0000001**	**5.88**	**±0.06**				

Note: Each $\delta^{18}O$ error (2σ) represents the counting statistics errors for each individual spot and the external error based on all standards during the session, which were added in quadrature.

Field aperture centering digits are given and show little difference between standard and sample. mount. The location of the unknowns is

Mount position X Y for standard and sample indicates that most analyses are within the central region to standards.

Weighted average uncertainties represent 2 standard deviations of the mean. The corresponding solution data are from:

91500: Wiedenbeck et al. (2004); OGC: Petersson et al. (2019); Penglai: Li et al., 2011; M257: Nasdala et al., 2008.

*Sequential order of analyses.

†Raw ratios drift corrected using the standard analyses versus time. The instrumental mass fractionation, corrected using alpha SIMS (ratio between the session average standard value and reference value).

§Session I was normalised to a $\delta^{18}O$ value of 9.86‰ for the 91500 standard and Session II to a $\delta^{18}O$ value of 5.31‰ for the Penglai standa

Table A5. Zircon Lu–Hf isotopes

Spot I.D	Corresponding U–Pb spot I.D	Spot size	No. ratios used	Comment	$^{176}Yb/^{177}Hf$	2σ	$^{176}Lu/^{177}Hf$	2σ	$^{176}Hf/^{177}Hf$	2σ	$^{178}Hf/^{177}Hf$	2σ	Interpreted age	σ	$^{207}Pb/^{206}Pb$ date	σ	ε_{Hft}*	2σ	$\delta^{18}O$	2σ
Session 1						±		±		±		±	(Ma)	± (Ma)	(Ma)	± (Ma)		±	(‰)	± (abs.)
PR1_15TKPB17_01b	n5932_15TKPB17-01b	40 µm	60/60	On U–Pb spo	0.0127	±0.0003	0.000446	±0.000003	0.280343	±.000018	1.467203	±0.000036	3704	±3	3704	±3	-2.4	±0.6	6.04	±0.30
PR1_15TKPB17_02a	n5932_15TKPB17-02a	40 µm	60/60	On U–Pb spo	0.0289	±0.0017	0.001066	±0.000074	0.280388	±.000025	1.467246	±0.000033	3632	±8	3632	±8	-4.1	±0.9	6.04	±0.31
PR1_15TKPB17_03	n5932_15TKPB17-03	40 µm	60/60	On U–Pb spo	0.0371	±0.0017	0.001184	±0.000028	0.280372	±.000029	1.467201	±0.000045	3732	±3	3732	±3	-2.6	±1.0	5.24	±0.29
PR1_15TKPB17_04b	n5932_15TKPB17-04b	40 µm	50/60	On U–Pb spo	0.0199	±0.0006	0.000703	±0.000006	0.280379	±.000023	1.467253	±0.000038	3710	±2	3710	±2	-1.7	±0.8		
PR1_15TKPB17_05	n5932_15TKPB17-05	40 µm	60/60	On U–Pb spo	0.0379	±0.0034	0.001270	±0.000113	0.280398	±.000028	1.467242	±0.000040	3699	±1	3699	±1	-2.7	±1.0		
PR1_15TKPB17_14	n5932_15TKPB17-14	40 µm	60/60	On U–Pb spo	0.0342	±0.0010	0.001136	±0.000046	0.280367	±.000026	1.467242	±0.000042	3713	±5	3713	±5	-3.1	±0.9		
PR1_15TKPB17_15a	n5932_15TKPB17-15a	40 µm	60/60	On U–Pb spo	0.0296	±0.0007	0.001099	±0.000021	0.280375	±.000028	1.467261	±0.000035	3729	±2	3729	±2	-2.4	±1.0	5.11	±0.30
PR1_15TKPB17_15b	n5932_15TKPB17-15b	40 µm	60/60	On U–Pb spo	0.0197	±0.0004	0.000738	±0.000005	0.280356	±.000019	1.467203	±0.000033	3735	±2	3735	±2	-2.0	±0.7	5.26	±0.31
PR1_15TKPB17_17	n5932_15TKPB17-17	40 µm	60/60	On U–Pb spo	0.0188	±0.0015	0.000577	±0.000040	0.280631	±.000024	1.467246	±0.000047	3451	±3	3457	±3	1.6	±0.9	*6.35*	*±0.30*
PR1_15TKPB17_19	n5932_15TKPB17-19	40 µm	45/60	On U–Pb spo	0.0261	±0.0031	0.000861	±0.000105	0.280639	±.000023	1.467258	±0.000042	3451	±3	3452	±3	1.2	±0.9	5.56	±0.34
PR1_15TKPB17_19b	n5932_15TKPB17-19	40 µm	60/60	Next to _19	0.0311	±0.0031	0.000998	±0.000109	0.280629	±.000029	1.467248	±0.000031	3451	±3	3452	±3	0.5	±1.1	5.56	±0.34
PR1_15TKPB17_41	n5932_15TKPB17-41	40 µm	60/60	On U–Pb spo	0.0201	±0.0002	0.000689	±0.000012	0.280337	±.000022	1.467210	±0.000042	3746	±3	3746	±3	-2.3	±0.8	*4.26*	*±0.30*
PR1_15TKPB17_s10	PR-10	40 µm	60/60	On U–Pb spo	0.0268	±0.0014	0.000914	±0.000050	0.280342	±.000024	1.467269	±0.000035	3696	±4	3696	±4	-3.9	±0.9		
PR3_15TKPB17_02	15tkpb17-02	40 µm	60/60	On U–Pb spo	0.0156	±0.0006	0.000560	±0.000006	0.280323	±.000021	1.467218	±0.000032	3731	±2	3731	±2	-2.8	±0.8	5.59	±0.46
PR3_15TKPB17_13	15tkpb17-13	35 µm	60/60	On U–Pb spo	0.0188	±0.0010	0.000631	±0.000019	0.280345	±.000034	1.467216	±0.000055	3681	±5	3681	±5	-3.4	±1.2		
PR3_15TKPB17_14	15tkpb17-14	40 µm	60/60	On U–Pb spo	0.0302	±0.0021	0.001039	±0.000089	0.280340	±.000028	1.467247	±0.000041	3689	±5	3689	±5	-4.4	±1.0		
PR3_18APPB12_02	18appb12-02	40 µm	35/60	On U–Pb spo	0.0439	±0.0035	0.001470	±0.000118	0.280406	±.000027	1.467229	±0.000036	3753	±3	3753	±3	-1.7	±1.0	*4.57*	*±0.57*
PR3_18APPB12_06	18appb12-06	40 µm	60/60	On U–Pb spo	0.0228	±0.0018	0.000742	±0.000045	0.280424	±.000024	1.467243	±0.000039	3463	±3	3463	±4	-5.9	±0.9	6.57	±0.47
PR3_18APPB12_08	18appb12-08	40 µm	60/60	On U–Pb spo	0.0044	±0.0001	0.000145	±0.000005	0.280578	±.000025	1.467214	±0.000044	3451	±3	3442	±7	0.7	±0.9	6.10	±0.43
PR3_18APPB12_10	18appb12-10	40 µm	35/60	On U–Pb spo	0.0128	±0.0004	0.000419	±0.000016	0.280592	±.000029	1.467299	±0.000059	3451	±3	3453	±4	0.6	±1.0	*6.08*	*±0.55*
PR3_18TKPB13_04	18appb13-04	40 µm	60/60	On U–Pb spo	0.0293	±0.0022	0.000930	±0.000047	0.280394	±.000028	1.467219	±0.000045	3729	±4	3729	±4	-1.3	±1.0	5.36	±0.45
PR3_18TKPB13_05	18appb13-05	40 µm	60/60	On U–Pb spo	0.0159	±0.0014	0.000516	±0.000038	0.280406	±.000026	1.467229	±0.000039	3650	±3	3650	±3	-1.7	±0.9	5.52	±0.49
PR3_18TKPB13_08	18appb13-08	40 µm	34/60	On U–Pb spo	0.0595	±0.0035	0.001721	±0.000124	0.280430	±.000037	1.467201	±0.000050	3675	±4	3675	±4	-3.3	±1.3	4.11	±0.50
PR3_18TKPB16_01	18appb16-01	40 µm	60/60	On U–Pb spo	0.0329	±0.0004	0.001159	±0.000007	0.280626	±.000027	1.467220	±0.000038	3696	±3	3696	±3	-2.9	±1.0	5.68	±0.45
PR3_18TKPB16_03	18appb16-03	40 µm	60/60	On U–Pb spo	0.0271	±0.0011	0.000914	±0.000038	0.280613	±.000027	1.467283	±0.000040	3451	±3	3456	±3	0.0	±1.0	6.37	±0.49
PR3_18TKPB16_03b	18appb16-03b	40 µm	60/60	On U–Pb spo	0.0490	±0.0016	0.001491	±0.000056	0.280409	±.000027	1.467248	±0.000041	3451	±3	3446	±3	0.1	±1.0	6.11	±0.47

Note: Present day value of CHUR $^{176}Hf/^{177}Hf = 0.282785$

Present day value of CHUR $^{176}Lu/^{177}Hf = 0.0336$

$\lambda = 1.867 \times 10^{-11}$

Itallic $d^{18}O$ denotes discarded analyses

In case of multiple O-isotope analyses in single grain, the value of the closest spot is denoted.

*ε_{Hft} calculated using the interpreted age of the rock.

Table A6. Zircon Lu–Hf standards

	$^{176}Hf/^{177}Hf$	2σ	$^{178}Hf/^{177}Hf$	2σ	$^{176}Lu/^{177}Hf$	2σ	$^{176}Yb/^{177}Hf$	2σ	Total Hf (V)	Comment
FC1										
	0.282182	±0.000018	1.467212	±0.000028	0.001672	±0.000001	0.05259	±0.000276	21.4	OK
	0.282167	±0.000016	1.467198	±0.000030	0.000630	±0.000000	0.01896	±0.000069	21.3	OK
	0.282175	±0.000017	1.467216	±0.000025	0.001452	±0.000005	0.04499	±0.000465	23.4	OK
	0.282185	±0.000018	1.467210	±0.000025	0.001458	±0.000019	0.04588	±0.000464	23.7	OK
	0.282177	±0.000020	1.467229	±0.000018	0.001869	±0.000030	0.05898	±0.000754	23.1	OK
	0.282201	±0.000022	1.467233	±0.000026	0.002681	±0.000014	0.08446	±0.000204	18.4	OK
	0.282182	±0.000022	1.467223	±0.000022	0.001700	±0.000007	0.05331	±0.000285	17.9	OK
	0.282185	±0.000018	1.467236	±0.000030	0.001215	±0.000004	0.03753	±0.000360	18.5	OK
	0.282170	±0.000019	1.467235	±0.000030	0.000982	±0.000001	0.02961	±0.000160	19.4	OK
	0.282182	±0.000019	1.467222	±0.000025	0.001184	±0.000004	0.03708	±0.000182	17.1	OK
Mean:	**0.282181**	**±0.000019**	**1.467221**	**±0.000026**	**0.001484**	**±0.000009**	**0.046339**	**±0.000322**		
Solution:	**0.282184**	**±0.000016**								
91500										
	0.282316	±0.000022	1.467200	±0.000046	0.000453	±0.000000	0.01322	±0.000077	9.4	OK
	0.282306	±0.000027	1.467250	±0.000036	0.000450	±0.000002	0.01333	±0.000105	9.2	OK
	0.282312	±0.000020	1.467210	±0.000040	0.000327	±0.000001	0.00927	±0.000029	10.2	OK
	0.282300	±0.000020	1.467222	±0.000040	0.000323	±0.000001	0.00967	±0.000201	9.7	OK
	0.282311	±0.000024	1.467251	±0.000036	0.000321	±0.000002	0.00913	±0.000049	9.4	OK
	0.282308	±0.000025	1.467250	±0.000039	0.000328	±0.000001	0.00941	±0.000083	9.4	OK
	0.282326	±0.000026	1.467214	±0.000044	0.000332	±0.000001	0.00944	±0.000060	9.1	OK
Mean:	**0.282311**	**±0.000024**	**1.467228**	**±0.000040**	**0.000362**	**±0.000001**	**0.010495**	**±0.000086**		
Solution:	**0.282306**	**±0.000008**								

OGC/OG1									$^{176}Hf/^{177}Hf_{(t)}$	2σ
	0.280598	±0.000019	1.467227	±0.000029	0.000639	±0.000035	0.01767 ±0.001092	16.9	OK	0.280555 ±0.000019
	0.280655	±0.000022	1.467221	±0.000030	0.001649	±0.000080	0.04857 ±0.003229	15.3	OK	0.280544 ±0.000022
	0.280643	±0.000022	1.467222	±0.000034	0.001057	±0.000008	0.02880 ±0.000181	16.7	OK	0.280573 ±0.000022
	0.280590	±0.000020	1.467211	±0.000026	0.000674	±0.000018	0.01800 ±0.000623	17.2	OK	0.280544 ±0.000020
	0.280641	±0.000018	1.467259	±0.000031	0.001263	±0.000049	0.03705 ±0.002159	15.2	OK	0.280556 ±0.000019
	0.280626	±0.000018	1.467231	±0.000030	0.000728	±0.000011	0.01977 ±0.000272	17.1	OK	0.280578 ±0.000018
	0.280641	±0.000023	1.467229	±0.000026	0.001049	±0.000012	0.03082 ±0.000277	14.4	OK	0.280571 ±0.000023
	0.280629	±0.000020	1.467230	±0.000034	0.001058	±0.000052	0.02944 ±0.001469	14.5	OK	0.280558 ±0.000021
	0.280630	±0.000022	1.467220	±0.000030	0.001434	±0.000066	0.04201 ±0.002580	14.5	OK	0.280534 ±0.000022
	0.280691	±0.000022	1.467232	±0.000039	0.001903	±0.000065	0.05508 ±0.002567	13.3	OK	0.280564 ±0.000023
Mean:	**0.280634**	**±0.000021**	**1.467228**	**±0.000031**	**0.001145**	**±0.000040**	**0.032721 ±0.001445**			**0.280558 ±0.000021**
Solution:	**0.280633**	**±0.000034**								**0.280554 ±0.000007**

Mud Tank								
	0.282482	±0.000011	1.467251	±0.000027	0.000011	±0.000000	0.00033 ±0.000006	18.8	OK
	0.282478	±0.000014	1.467220	±0.000025	0.000008	±0.000000	0.00026 ±0.000008	18.3	OK
	0.282490	±0.000013	1.467231	±0.000027	0.000008	±0.000000	0.00027 ±0.000007	18.6	OK
	0.282491	±0.000013	1.467257	±0.000025	0.000010	±0.000000	0.00033 ±0.000006	18.8	OK
	0.282480	±0.000011	1.467251	±0.000027	0.000008	±0.000000	0.00026 ±0.000007	18.5	OK
	0.282488	±0.000014	1.467228	±0.000027	0.000009	±0.000000	0.00027 ±0.000009	18.0	OK
	0.282494	±0.000016	1.467259	±0.000026	0.000008	±0.000000	0.00025 ±0.000009	18.5	OK
	0.282478	±0.000013	1.467222	±0.000026	0.000008	±0.000000	0.00026 ±0.000007	17.6	OK
	0.282488	±0.000013	1.467223	±0.000031	0.000008	±0.000000	0.00026 ±0.000006	18.0	OK
	0.282487	±0.000014	1.467232	±0.000032	0.000008	±0.000000	0.00026 ±0.000007	18.2	OK
	0.282487	±0.000017	1.467237	±0.000023	0.000010	±0.000000	0.00032 ±0.000007	18.1	OK
	0.282493	±0.000014	1.467239	±0.000029	0.000008	±0.000000	0.00027 ±0.000008	18.3	OK
	0.282493	±0.000014	1.467224	±0.000029	0.000008	±0.000000	0.00027 ±0.000008	18.5	OK
	0.282496	±0.000014	1.467219	±0.000027	0.000008	±0.000000	0.00026 ±0.000007	18.7	OK
	0.282489	±0.000013	1.467233	±0.000029	0.000008	±0.000000	0.00026 ±0.000007	18.2	OK
Mean:	**0.282488**	**±0.000014**	**1.467235**	**±0.000027**	**0.000009**	**±0.000000**	**0.000276 ±0.000007**		
Solution:	**0.282507**	**±0.000006**							

Note: Summary of Lu–Hf–Yb isotope data measured from reference zircons during the course of this study by laser ablation MC-ICPMS, where Hf isotope ratios are session normalized to Mud Tank zircon $^{176}Hf/^{177}Hf$=0.282507 (Woodhead and Hergt, 2005, itself reported relative to JMC475 $^{176}Hf/^{177}Hf$=0.282160). Uncertainties represent 2 standard deviations of the mean. The corresponding solution data are from:
FC-1: $^{176}Hf/^{177}Hf$=0.282184±0.000016, Temora 2 $^{176}Hf/^{177}Hf$=0.282686±0.000008, 91500 $^{176}Hf/^{177}Hf$=0.282306±0.000008 (Woodhead and Hergt, 2005), and OGC $^{176}Hf/^{177}Hf$=0.280633±0.000034 (Kemp et al., 2017). All reported relative to JMC475 $^{176}Hf/^{177}Hf$ =0.282160.